NASA Technical Memorandum 87812

Tidal Estimation in the Atlantic and Indian Oceans, 3° x 3° Solution

Braulio V. Sanchez, Desiraju B. Rao,
and Stephen D. Steenrod

APRIL 1987

NASA

NASA Technical Memorandum 87812

Tidal Estimation in the Atlantic and Indian Oceans, 3° x 3° Solution

Braulio V. Sanchez
Goddard Space Flight Center
Greenbelt, Maryland

Desiraju B. Rao
National Oceanic and Atmospheric Administration
National Meteorological Center
Rockville, Maryland

Stephen D. Steenrod
Applied Research Corporation
Landover, Maryland

NASA
National Aeronautics
and Space Administration

Scientific and Technical
Information Branch

1987

I. INTRODUCTION

The extraction of ocean tidal components from the analysis of satellite altimetry data could become an alternative and complementary method to the numerical integration of the Laplace tidal equations.

Mazzega (1985) created a global model of the M2 tide using twenty-four days of SEASAT altimetry data; the solution was obtained by means of surface spherical harmonics; the results were qualitatively realistic. No hydrodynamic equations were used.

Woodworth, P.L. and Cartwright, D.E. (1986) have extracted the M2 ocean tide from SEASAT altimetry data. They used three complementary methods. The first method provides point measurements of the tide at the crossovers of the SEASAT repeat orbit ground track; it was applied in the tropical ocean areas. The other two methods involve the spatial expansion of M2 in terms of either surface spherical harmonics or Platzman normal modes of the world ocean. The results reproduce many features of the tide represented in recent tidal models.

The purpose of this investigation is to develop an estimation technique which will serve to extrapolate tidal amplitudes and phases over entire ocean basins using existing gauge data and the precise altimetric measurements which are now beginning to be provided by satellite oceanography. The applicability of the extrapolating technique was tested in the Lake Superior basin by Sanchez, Rao and Wolfson (1985) and in the Atlantic-Indian Oceans (using a $6^\circ \times 6^\circ$ degree) by Sanchez, Rao and Steenrod (1986 a, b).

The method to be used in this investigation requires several distinct steps. First it is necessary to determine numerically the stream function and velocity potential orthogonal functions (The Stokes/Helmholtz Potentials) which span the space of the basin under consideration. These space functions are then used in the Laplace tidal equations to determine the homogeneous solution (normal modes) and the forced solution. The latter is obtained by adding the astronomical forcing function modified to include solid-earth tides.

The velocity potential eigenfunctions obtained as a first step are used also to extrapolate the surface height field over the entire space domain of the given basin and this approach will constitute a distinct and integral part of the investigation.

The theoretical foundation is Proudman's theory (1918) as formulated by Rao (1966). The theory provides the formalism for calculation of the gravitational (first class) normal modes and the rotational (second class or Rossby waves) normal models of irregularly shaped basins with realistic bathymetry.

The method requires the solution of two elliptic partial differential equations with second order operators which are simpler than the tidal operator. The boundary conditions correspond to vanishing of the stream function and normal derivative of the velocity potential. The elliptic operators are represented numerically in finite difference form, the grid used is a Richardson lattice which preserves self-adjointness. The solutions yield the velocity and surface height fields in terms of orthogonal functions with time-dependent coefficients. These functions are then substituted into the Laplace's tidal equations: if the homogeneous equations are used one obtains the normal modes; if the forcing terms are included then the forced solution is obtained. In both cases the solution is obtained numerically. The surface height field is only dependent on the velocity potential orthogonal functions. The expansion coefficients of these functions can be estimated in a least-square sense from available selected tidal measurements.

2. BASIC EQUATIONS

Free Solutions

The method of approach was developed originally by Proudman (1918) using a Lagrangian approach. It was reformulated by Rao (1966) from the Eulerian point of view. The basic ideas of the method presented below follow Rao's line of development. The basic equations are the linearized shallow water equations on a rotating plane:

$$\frac{\partial \vec{M}}{\partial t} - f[\vec{M}] = -g\,\overline{H} h\,\nabla\eta$$
$$\frac{\partial \eta}{\partial t} + \nabla \cdot \vec{M} = 0 \tag{2.1}$$

where

$$\vec{M} \equiv H\vec{V} \equiv (M,N)$$

$$\vec{V} \equiv (u,v)$$

$$f \equiv 2\omega \sin\theta$$

$$h(x,y) \equiv H(x,y)/\overline{H}.$$

H(x,y) is the variable depth of the fluid in equilibrium and $\overline{H}$ is some constant scaling depth, f is the Coriolis parameter, $\vec{V}$ is the horizontal velocity vector, η the fluctuation of the free surface. g is the apparent gravitational acceleration and ∇ is the horizontal gradient operator. []: denotes rotation of the vector through a right angle in the clockwise direction of the horizontal plane, i.e. $[] = -(\vec{k} \times \nabla)$, $\vec{k}$ being a unit vector vertical to the horizontal plane.

The appropriate boundary conditions to be adjoined to equations (2.1) are

$$\vec{M} \cdot \vec{n} = 0 \tag{2.2}$$

on the coast, where $\vec{n}$ is the unit normal to the coastline.

The transport vector $\vec{M}$ may be partitioned as follows:

$$\vec{M} = \vec{M}^{\phi} + \vec{M}^{\psi} \tag{2.3}$$

where

$$\vec{M}^{\phi} = -h\,\nabla\phi$$

$$\vec{M}^{\psi} = -[\nabla\psi] \tag{2.4}$$

$\vec{M}^{\psi}$ is the solenoidal part of $\vec{M}$ while $h^{-1}\vec{M}^{\phi}$ is the irrotational part since

$$\nabla\cdot[h^{-1}\vec{M}^{\phi}] = 0$$

$$\nabla\cdot\vec{M}^{\psi} = 0$$

To complete the determination of ϕ and ψ, it is necessary to specify the boundary conditions $\vec{M}^{\phi} \cdot \vec{n} = 0$ and $M^{\psi} \cdot \vec{n} = 0$ to ensure that Eq. (2.2) is satisfied. In terms of ϕ and ψ the conditions then are

$$h\frac{\partial\phi}{\partial n} = 0 \tag{2.5}$$

and

$$\psi = 0$$

on the boundaries. The divergence of the transport field and the vorticity of the velocity field yield

$$\nabla \cdot \vec{M} = -\nabla \cdot h \nabla \phi$$

$$\nabla \cdot [h^{-1}\vec{M}] = \nabla \cdot h^{-1} \nabla \psi \tag{2.6}$$

If $\vec{M}$ is known as a function of the horizontal coordinates, the left-sides of (2.6) are specified. Then each equation represents an inhomogeneous elliptic differential equation with homogeneous boundary conditions given by Eq. (2.5), and it is well known that such problems possess a unique solution. It is also straightforward to prove that the representation of $\vec{M}$ as given in Eqs. (2.3, 4, 5) is unique. Since $\vec{M}$ itself is unknown, the procedure then consists of expanding ϕ and ψ in terms of the spectra of the elliptic operators appearing in Eqs. (2.6); that is, we seek solutions which satisfy the following equations

$$\begin{aligned} \nabla \cdot h \nabla \phi_\gamma &= -\lambda_\gamma \phi \\ \nabla \cdot h^{-1} \nabla \psi_\gamma &= -\mu_\gamma \psi_\gamma \end{aligned} \tag{2.7}$$

where ϕ_γ, ψ_γ are the characteristic functions and λ_γ, μ_γ are the characteristic values associated with the corresponding operators $\nabla \cdot h \nabla$ and $\nabla \cdot h^{-1} \nabla$. The characteristic functions satisfy the boundary conditions

$$\begin{aligned} h \frac{\partial \phi_\gamma}{\partial n} &= 0 \\ h^{-1} \psi_\gamma &= 0 \end{aligned} \tag{2.8}$$

The condition $h^{-1}\psi_\gamma = 0$ imposes a stronger condition than that required by (2.5). However, the factor h^{-1} is necessary to make the ψ_γ problem self-adjoint. Since the problems (2.7, 8) are self-adjoint, the characteristic values of λ_γ and μ_γ are real and the characteristic functions ϕ_γ and ψ_γ each constitute a complete and internally orthogonal set. Without loss of generality, the orthogonality condition may be chosen as:

$$\begin{aligned} \int h^{-1} \vec{M}_\gamma^\phi \cdot \vec{M}_\beta^\phi dA &= \lambda_\gamma \int \phi_\gamma \phi_\beta dA = Ac^2 \overline{H}^2 \delta_{\gamma\beta}, \\ \int h^{-1} \vec{M}_\gamma^\psi \cdot \vec{M}_\beta^\psi dA &= \lambda_\gamma \int \psi_\gamma \psi_\beta dA = Ac^2 \overline{H}^2 \delta_{\gamma\beta}, \end{aligned} \tag{2.9}$$

where $c^2 = gH$ and A is the surface area of the basin. $\delta_{\gamma\beta}$ is the Kronecker delta. We have further defined, in accordance with (2.4),

$$\vec{M}_\gamma^\phi = -h \nabla \phi_\gamma \text{ and } \vec{M}_\gamma^\psi = -[\nabla \psi_\gamma]$$

in the orthogonality condition (2.9).

The components of the transport vector can now be represented by the sums

$$\begin{aligned} \vec{M}^\phi &= \sum_\gamma P_\gamma \vec{M}_\gamma^\phi, \\ \vec{M}^\psi &= \sum_\gamma Q_\gamma \vec{M}_\gamma^\psi, \end{aligned} \tag{2.10}$$

where P_γ and Q_γ are the expansion coefficients. The orthogonality conditions ensure that equations (2.10) represent the least squares approximations to $\vec{M}^\phi$ and $\vec{M}^\Psi$ if and when the sums span the complete spectra of equations (2.7). The height field η is governed by the divergent part of M and the ϕ_γ functions yield a sufficient basis for its representation. A convenient representation for η may be taken as:

$$\begin{aligned} \eta &= \sum_\gamma R_\gamma \eta_\gamma, \\ \eta_\gamma &= c^{-1}(\lambda_\gamma)^{1/2}\phi_\gamma, \end{aligned} \tag{2.11}$$

where R_γ are the expansion coefficients for the η-field.

Substitution of equations (2.10) and (2.11) into equations (2.1) and the use of the orthogonality conditions (2.9) yield a set of prediction equations for the expansion coefficients:

$$\begin{aligned} \frac{dP_\gamma}{dt} - \sum_\beta A_{\gamma\beta}P_\beta - \sum_\beta B_{\gamma\beta}Q_\beta - \vartheta_\gamma R_\gamma &= 0 \\ \frac{dQ_\gamma}{dt} - \sum_\beta C_{\gamma\beta}P_\beta - \sum_\beta D_{\gamma\beta}Q_\beta &= 0 \\ \frac{dR_\gamma}{dt} + \vartheta_\gamma P_\gamma &= 0 \end{aligned} \tag{2.12}$$

where the coupling coefficients are given by

$$\begin{aligned} A_{\gamma\beta} &\equiv \{\vec{M}^\phi_\gamma, [\vec{M}^\phi_\beta]\}, & B_{\gamma\beta} &\equiv \{\vec{M}^\phi_\gamma, [\vec{M}^\Psi_\beta]\}, \\ C_{\gamma\beta} &\equiv \{\vec{M}^\Psi_\gamma, [\vec{M}^\phi_\beta]\}, & D_{\gamma\beta} &\equiv \{\vec{M}^\Psi_\gamma, [\vec{M}^\Psi_\beta]\}, \end{aligned} \tag{2.13}$$

The quantity inside the angular brackets represents an inner product of two vectors $\vec{W}$ and $\vec{T}$ and is denoted by

$$\{\vec{W},\vec{T}\} = (1/c^2\, A\overline{H}^2) \int_A fh^{-1}\, \vec{W}\cdot\vec{T}dA.$$

It can be seen from Eq. (2.12, 13) and the definition of the inner product that all the coupling coefficients vanish when the Coriolis parameter $f = 0$ and hence

$$\frac{d^2P_\gamma}{dt^2} + \vartheta^2{}_\gamma P_\gamma = 0.$$

$\vartheta_\gamma = (c^2\lambda_\gamma)^{1/2}$, is the non-rotating frequency of oscillation. In equations (2.12, 13) the subscript γ (or β) is used as a proxy for a binary index and represents an ordering of the characteristic functions ϕ_γ, ψ_γ in some as yet unspecified manner. For convenience we replace the wavenumber index γ by scalar indices i = 1,2,3 (or j = 1,2,3 . . .) and denote

$$\begin{aligned} \lambda_i &\equiv \lambda_{\gamma i},\ M_i \equiv M_{\gamma i},\ \vartheta_i \equiv \vartheta_{\gamma i} \\ P_i &\equiv P_{\gamma i},\ \equiv Q_{\gamma i},\ R_i \equiv R_{\gamma i} \\ A_{ij} &\equiv A_{\gamma i\beta j} \\ B_{ij} &\equiv B_{\gamma i\beta j} \\ C_{ij} &\equiv C_{\gamma i\beta j} \\ D_{ij} &\equiv D_{\gamma i\beta j} \end{aligned} \tag{2.14}$$

Using the above notation, we can define column vectors

$$\overset{\bullet}{P} \equiv \text{col}\ (P_i),\ \overset{\bullet}{Q} = \text{col}\ (Q_i),\ \overset{\bullet}{R} = \text{col}\ (R_i)$$

$$S \equiv \begin{vmatrix} \overset{\bullet}{P} \\ \overset{\bullet}{Q} \\ \overset{\bullet}{R} \end{vmatrix} \tag{2.15a}$$

and matrices

$$\underset{\sim}{A} \equiv \{ A_{ij} \},\ \underset{\sim}{B} \equiv \{ B_{ij} \}$$

$$\underset{\sim}{C} \equiv \{ C_{ij} \},\ \underset{\sim}{D} \equiv \{ D_{ij} \} \tag{2.15b}$$

$$\langle \vartheta \rangle \equiv \text{diagonal}\ \vartheta_i$$

Equations (2.12) may now be written in the form

$$\frac{d\overset{\bullet}{s}}{dt} + \underset{\sim}{a}\ \overset{\bullet}{s} = 0 \tag{2.16}$$

where $\underset{\sim}{a}$ is the square matrix

$$\underset{\sim}{a} \equiv \begin{vmatrix} -A & -B & -\langle \vartheta \rangle \\ -C & -D & 0 \\ \langle \vartheta \rangle & 0 & 0 \end{vmatrix} \tag{2.17}$$

In seeking the solutions for the normal modes, we assume

$$\vec{s} \sim e^{i\sigma t}$$

where σ is the normal mode frequency with rotation and $i \equiv \sqrt{-1}$. Eq. (2.15) then reduces to

$$(\sigma \mathrm{II} - i\underset{\sim}{a})\ \vec{s} = 0. \tag{2.18}$$

In the preceding equation II is the identity matrix. σ's are the characteristic values of the matrix $i\underset{\sim}{a}$. From the definition of the coupling coefficients given in (2.13) and the matrix $\underset{\sim}{a}$ as defined in (2.17), it is clear that $i\underset{\sim}{a}$ exhibits Hermitian symmetry and hence the σ's constitute a spectrum of real eigenvalues. In computing the matrix elements in $\underset{\sim}{a}$, the basis functions ϕ_i and ψ_i are chosen to correspond to an ordering of the characteristic values λ_i and μ_i arranged so that $\lambda_1 < \lambda_2 < \lambda_3 \ldots$ and $\mu_1 < \mu_2 < \mu_3 \ldots$. Such an ordering has been chosen since the λ_i's and μ_i's have the dimensions of (wavenumber)^2. Hence, at any order of truncation, those ϕ_i's and ψ_i's with the largest space scales are taken into account.

Forced Solution

In the computation of the forced solution we include the effects of the yielding of the solid earth to tide generating forces. The effects due to self-attraction of the tide and tidal loading as well as the frictional effects have not been included. The theory allows for the inclusion of these effects but they introduce computational complications and physical uncertainties and they are not necessary in the context of the application of the interpolation technique. Equations (2.1) are recast for the forced tidal oscillations as

$$\frac{\partial \vec{M}}{\partial t} - f[\overset{\bullet}{M}] = -g\bar{H}h\nabla\eta',$$
$$\frac{\partial \eta}{\partial t} + \nabla.\overset{\bullet}{M} = 0, \tag{2.19}$$

where

$$\eta' = \eta - (1 + k_2 - h_2)\bar{\eta}.$$

k_2, h_2 are the Love numbers and $\bar{\eta}$ is the equilibrium tide height. Let the vector $\vec{G} = g\bar{H}h\,(1+k_2-h_2)\nabla\bar{\eta}$. Equations (2.19) can then be written

$$\frac{\partial \vec{M}}{\partial t} - f[\vec{M}] = -g\bar{H}h\nabla\eta + \vec{G}$$
$$\frac{\partial \eta}{\partial t} + \nabla.\vec{M} = 0, \tag{2.20}$$

Substitution of the expansions (2.10) and (2.11) into equations (2.20) yields, after using (2.13)

$$\frac{dP_\gamma}{dt} - \sum_\beta A_{\gamma\beta}P_\beta - \sum_\beta B_{\gamma\beta}Q_\beta - \vartheta_\gamma R_\gamma = (c^2A\bar{H}^2)^{-1}\int fh^{-1}\vec{G}\cdot\vec{M}_\gamma^\phi dA$$
$$\frac{dQ_\gamma}{dt} - \sum_\beta C_{\gamma\beta}P_\beta - \sum_\beta D_{\gamma\beta}Q_\beta = (c^2A\bar{H}^2)^{-1}\int fh^{-1}\vec{G}\cdot\vec{M}_\gamma^\psi\,dA \tag{2.21}$$
$$\frac{dR_\gamma}{dt} + \vartheta_\gamma P_\gamma = 0$$

Define the vector $\overset{\bullet}{F}$ as follows,

$$\overset{\bullet}{F} = \begin{vmatrix} (c^2A\bar{H}^2)^{-1}\int fh^{-1}\vec{G}\cdot\vec{M}_\gamma^\phi dA \\ (c^2A\bar{H}^2)^{-1}\int fh^{-1}\vec{G}\cdot\vec{M}_\gamma^\phi dA \\ 0 \end{vmatrix} \tag{2.22}$$

Equations (2.21) can then be written as an inhomogeneous matrix equation

$$\frac{d\overset{\bullet}{S}}{dt} + \underset{\sim}{a}\vec{S} = \vec{F}, \tag{2.23}$$

where $\overset{\bullet}{S}$ and $\underset{\sim}{a}$ are defined by equations (2.15a) and (2.17). The solution of equation (2.23) is given by

$$\vec{S} = \underset{\sim}{C}\langle e^{i\sigma t}\rangle\int_0^t \langle e^{-i\sigma\tau}\rangle \underset{\sim}{C}^{-1}\vec{F}(\tau)\,d\tau, \tag{2.24}$$

where C is the modal matrix containing the eigenvectors of $\underset{\sim}{a}$ arranged in columns and σ are the characteristics values of $\underset{\sim}{a}$. $\langle e^{i\sigma t}\rangle$ is a diagonal matrix.

3. ESTIMATION

The orthogonal functions ϕ_γ form a basis for the expansion of the height field η, as discussed earlier. Since these functions are characteristic for a particular basin and are described at all points inside the basin (within the resolution of the finite difference grid), they can be used as optimal functions for extrapolation of the tidal field over the whole basin, given data at some selected points.

Eventhough the basis functions are orthogonal, in fitting the data to these functions it is preferable to use linear least-squares techniques to determine the coefficients of expansion rather than the orthogonality property since real data are not

usually available at regularly spaced points. A similar approach was taken in a previous investigation by Rao and Schwab (1981) in which they determined the steady circulation in a closed basin for which the appropriate orthogonal functions are the ψ_γ functions and Sanchez et al. (1985) used the ϕ_γ functions for tidal extrapolation in Lake Superior. An outline of the procedure and the basic equations involved are given below.

The tidal height field as given by equations (2.11) and (2.15) can be written

$$\eta(x,y,t) = \sum_\gamma R_{\gamma r}\, \eta_\gamma(x,y)\, \cos\sigma t - \sum_\gamma R_{\gamma I}\, \eta_\gamma(x,y)\, \sin\sigma t \tag{3.1}$$

where $R_{\gamma r}$ and $R_{\gamma I}$ denote the real and imaginary parts of R_γ. The tidal height field can be expressed also in terms of amplitude $A(x,y)$ and phase $\Theta(x,y)$, that is

$$\eta(x,y,t) = A(x,y)\, \cos\,[\sigma t - \Theta(x,y)] \tag{3.2}$$

Comparing equations (3.1) and (3.2) one obtains the following relations,

$$\begin{aligned} A(x,y) &= [(\sum_\gamma R_{\gamma r}\, \eta_\gamma)^2 + (\sum_\gamma R_{\gamma I}\, \eta_\gamma)^2]^{1/2} \\ \Theta(x,y) &= \text{arc tan}\, [-(\sum_\gamma R_{\gamma I}\, \eta_\gamma)/(\sum_\gamma R_{\gamma r}\, \eta_\gamma)] \end{aligned} \tag{3.3}$$

Also, from equations (3.1) and (3.2) one obtains the following vector-matrix relations

$$\begin{aligned} [\underset{\sim}{\eta}]\, \overset{\bullet}{R}_r &= \overset{\bullet}{A} \cos\Theta \\ [\underset{\sim}{\eta}]\, \overset{\bullet}{R}_I &= \overset{\bullet}{A} \sin\Theta \end{aligned} \tag{3.4}$$

The components of the vectors $\overset{\bullet}{A}\cos\Theta$ and $\overset{\bullet}{A}\sin\Theta$ are the "n" available tidal measurements. The matrix $[\underset{\sim}{\eta}]$ is available from the solution of the velocity potential eigenfunctions, its "k" columns will correspond to the velocity potential eigenfunctions chosen to represent the forced solution, its "n" rows correspond to the location of the tidal measurements in the basin under consideration. The least squares solution to equations (3.4) is then given by

$$\begin{aligned} \overset{\bullet}{R}_r &= ([\underset{\sim}{\eta}]^T[\underset{\sim}{\eta}])^{-1}[\underset{\sim}{\eta}]^T\, \overset{\bullet}{A}\ \cos\Theta, \\ \overset{\bullet}{R}_I &= ([\underset{\sim}{\eta}]^T[\underset{\sim}{\eta}])^{-1}[\underset{\sim}{\eta}]^T\, \overset{\bullet}{A}\ \sin\Theta, \end{aligned} \tag{3.5}$$

where $[\underset{\sim}{\eta}]^T$ is the transposed matrix. Having determined a certain number of coefficients $\overset{\bullet}{R}_r$ and $\overset{\bullet}{R}_I$, since the functions $\eta_\gamma(x,y)$ are known over the entire basin, one can obtain the amplitude and phase of the tidal height at all points in the basin from eq. (3.3). The maximum number of coefficients $\overset{\bullet}{R}_r$ and $\overset{\bullet}{R}_I$ that can be determined will be the same as the number of observations available.

4. RESULTS

Normal Modes and Forced Solutions

A normal mode solution for the Atlantic and Indian Oceans has been obtained by means of a 3° x 3° finite difference grid. There are 1915 velocity potential and 1717 stream function points distributed such as to form a single Richardson lattice. A finite difference solution of equations (2.7) subject to the boundary conditions given by equations (2.8) yields the eigenvalues and eigenvectors for both fields. The eigenfunctions of the ϕ solution represent the non-rotating gravitational normal modes of the basin, the periods of oscillation of the lowest modes are given in the first column of Table 1. The stream function modes generate the vorticity component of the flow field in the rotating case for the gravitational and rotational species, they are more dominant for the quasi-geostrophic rotational modes than for the gravitational modes. The normal mode solution was obtained by including the lowest 150 eigenfunctions from each field (ϕ and ψ) into the dynamical equations, the solution of the eigenvalue problem posed by equation (2.18) yields the normal modes. The normal modes fall into two distinct categories: the inertia-gravitational modified by rotation and the rotational modified by divergence. If the secular determinant is truncated at a size n x n, then one obtains 2n/3 gravitational modes and n/3 rotational modes, in pairs (plus and minus the same value). In our case there are 300 gravitational modes and 150 rotational modes. The rotational modes are characterized

by high ratios of kinetic to potential energy; these modes will vanish in a basin of constant depth and Coriolis parameter. The rotational normal modes are extremely sensitive to the resolution of the shape of the basin and the bottom topography and the convergence of their roots is more complicated than for gravitational modes. A detailed discussion of the nature of the two types of modes is given by Platzman (1975) and Rao and Schwab (1976). The gravitational modes are by far the most important in the context of the diurnal and semidiurnal tides as shown by Platzman (1984).

Table 1 presents a list of the first 20 gravitational modes in order of decreasing period. Both the non-rotational and rotational values are given, the non-rotational gravity modes are equivalent to the eigenfunctions of the velocity potential or

TABLE 1. GRAVITATIONAL MODES

PERIOD (hours) NON-ROTATIONAL		PERIOD (hours) ROTATIONAL		ENERGY RATIO (KINETIC/POTENTIAL)	
3° x 3°	6° x 6°	3° x 3°	6° x 6°	3° x 3°	6° x 6°
81.20		68.14		1.66	
	77.68		67.92		1.47
42.19		43.99		0.93	
	40.98		42.53		0.96
29.23		31.16		0.79	
29.03		29.20		0.94	
	29.00		29.61		0.81
28.21		28.20		0.94	
	22.17		23.55		0.84
22.13		22.89		0.90	
20.79		20.61		0.87	
	20.73		20.93		0.86
19.31		19.13		1.20	
	19.20		19.40		1.19
18.94		17.59		0.99	
	16.52		17.34		1.03
16.29		16.21		0.92	
15.34		15.51		1.05	
14.76		14.79		0.89	
	14.56		15.73		1.11
	14.17		14.44		0.86
14.05		13.68		0.98	
	13.42		13.93		1.03
13.13		12.85		1.05	
	12.94		12.99		1.07
12.89		12.68		1.05	
	12.74		12.55		1.27
12.25		12.05		1.15	
12.18		11.88		1.03	
11.73		11.55		1.03	
	11.72		11.99		1.09
11.57		11.10		1.01	
	11.47		11.13		1.14
11.30		10.96		1.11	

Proudman functions. The last entry is the ratio of energies (kinetic/potential). Table 1 gives the values obtained with the 3° x 3° grid as well as the results previously obtained with a 6° x 6° grid (1986 a, b). Notice that in the range covered there are only 14 values for the 6° x 6° grid as compared to 20 for the finer 3° x 3° mesh; this is to be expected.

Table 2 lists the 20 most powerful modes for the M2 and K1 tidal components in order of decreasing power. The entries in the table give the power ranking, the rotational period in hours, the percentage of the total power for that mode and the percentage of the total power contributed by all the modes included up to that point.

TABLE 2. POWER SPECTRUM FOR THE M2 AND K1 COMPONENTS.

	M2			K1		
RANK	PERIOD (HOURS)	POWER (%) EACH	SUM	PERIOD (HOURS)	POWER (%) EACH	SUM
1	12.68	7.73	7.73	22.89	10.47	10.47
2	11.10	5.76	13.50	19.13	6.88	17.36
3	11.55	5.23	18.73	20.61	6.57	23.94
4	10.96	5.08	23.82	13.68	4.50	28.44
5	10.26	3.17	27.00	17.59	4.43	32.88
6	11.88	2.97	29.98	16.21	4.41	37.30
7	8.79	2.93	32.91	12.85	4.12	41.43
8	9.67	2.61	35.53	68.14	2.53	43.97
9	10.37	2.54	38.07	10.96	2.47	46.44
10	10.13	2.26	40.33	12.05	2.42	48.87
11	9.26	2.23	42.57	28.20	2.09	50.96
12	10.52	2.16	44.74	29.20	2.06	53.03
13	14.79	2.10	46.84	11.55	2.01	55.05
14	9.49	1.99	48.84	10.52	1.98	57.03
15	12.05	1.94	50.79	31.16	1.81	58.84
16	12.85	1.90	52.69	9.49	1.79	60.63
17	13.68	1.88	54.57	15.51	1.42	62.06
18	8.42	1.74	56.32	12.68	1.41	63.48
19	20.61	1.70	58.02	9.26	1.39	64.87
20	10.02	1.65	59.68	43.99	1.27	66.15

The three most powerful modes in the M2 spectrum are the modes with periods of 12.68 hours (7.73%), 11.10 hours (5.76%) and 11.55 hours (5.23%). For the K1 spectrum the three most powerful modes have periods of 22.89 hours (10.47%), 19.13 hours (6.88%) and 20.61 hours (6.57%). Figures 1 to 6 below give the structure (amplitude and phase) for these 6 modes. The amplitudes have been normalized to a maximum value of 100; the amplitude contours are shown by the solid lines and the dotted lines correspond to the phases.

Figures 7 and 8 show the M2 and K1 tidal solutions. These solutions were obtained by including the first 150 eigenfunctions from the ϕ and ψ solutions. The forced solution for η then contains 150 coefficients R_γ. The contours of equal amplitude and phase are given by the solid and dotted lines respectively. The arrows indicate the sense of progression for high and low water. The M2 solution has an amplitude RMS of 53.4 cm; the corresponding value for K1 is 10.0 cm.

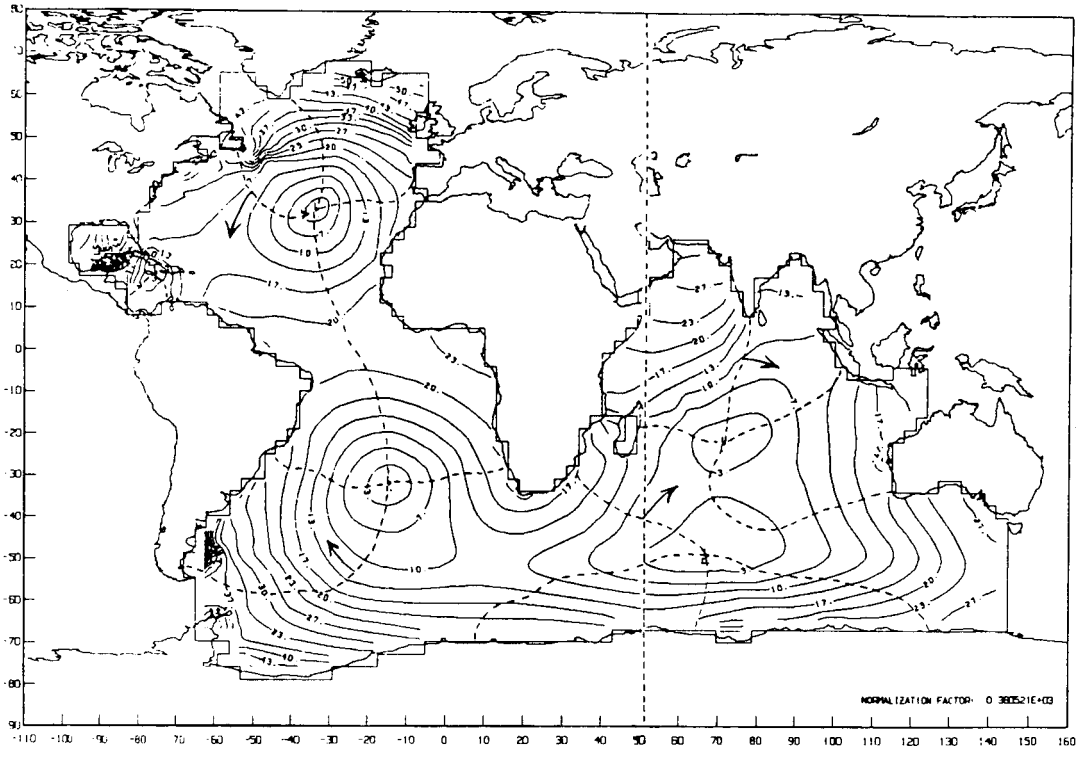

Figure 1. Normal Mode, Period = 22.89 Hours

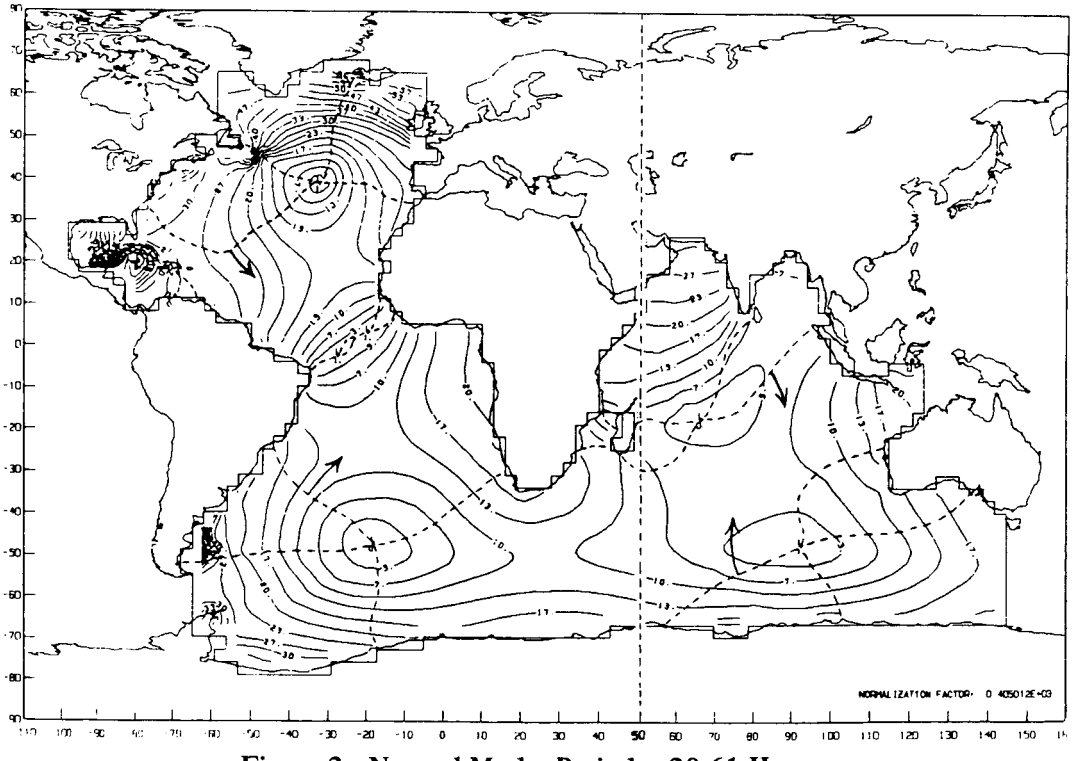

Figure 2. Normal Mode, Period = 20.61 Hours

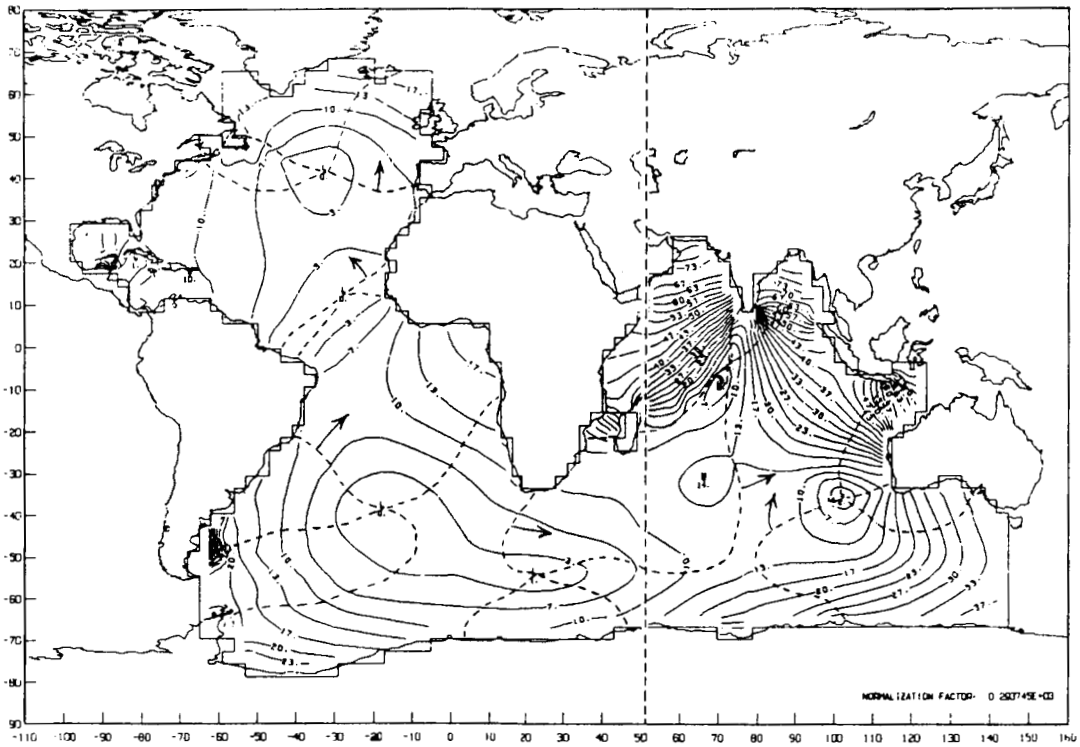

Figure 3. Normal Mode, Period = 19.13 Hours

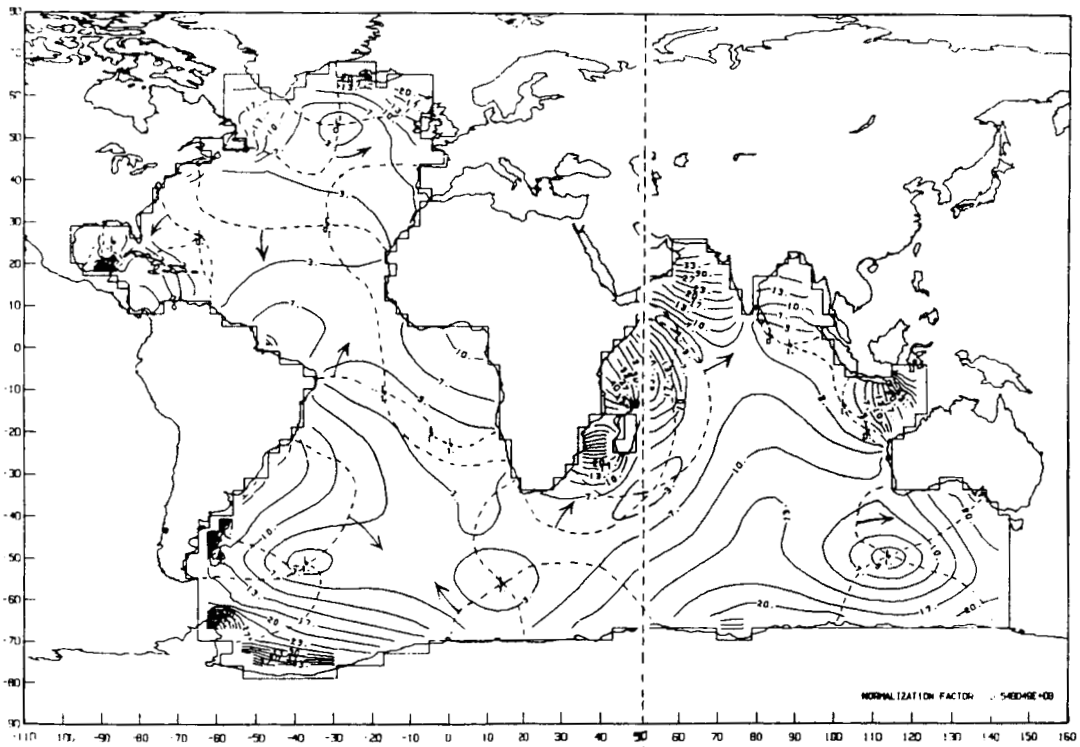

Figure 4. Normal Mode, Period = 12.68 Hours

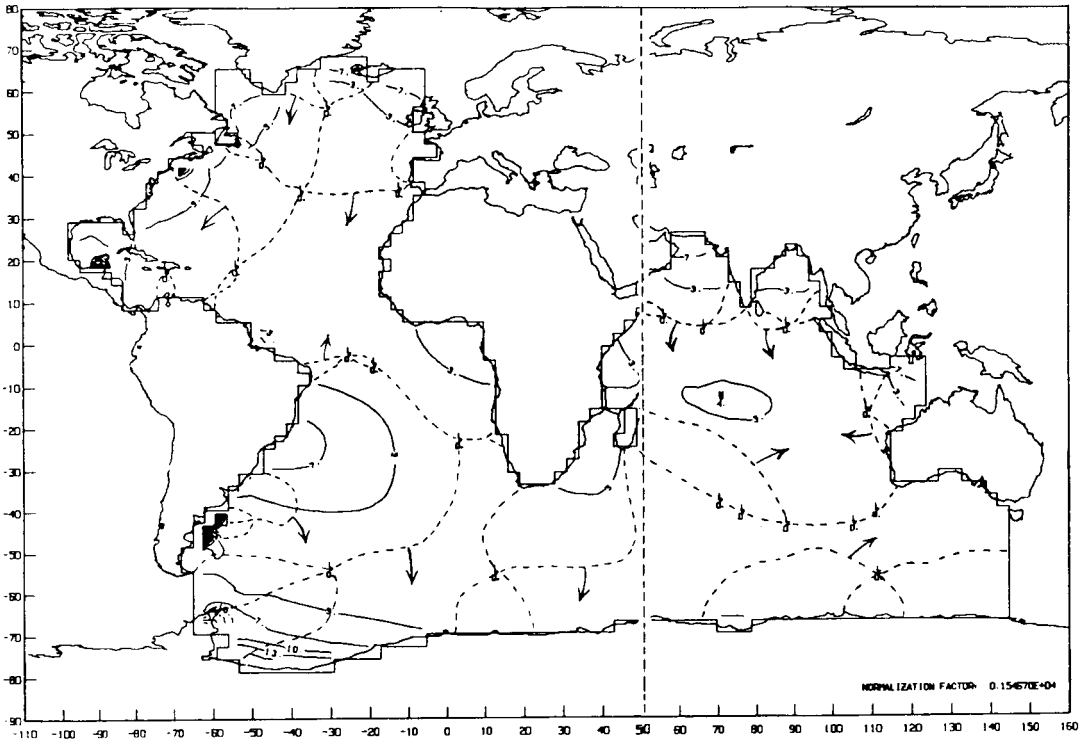

Figure 5. Normal Mode, Period = 11.55 Hours

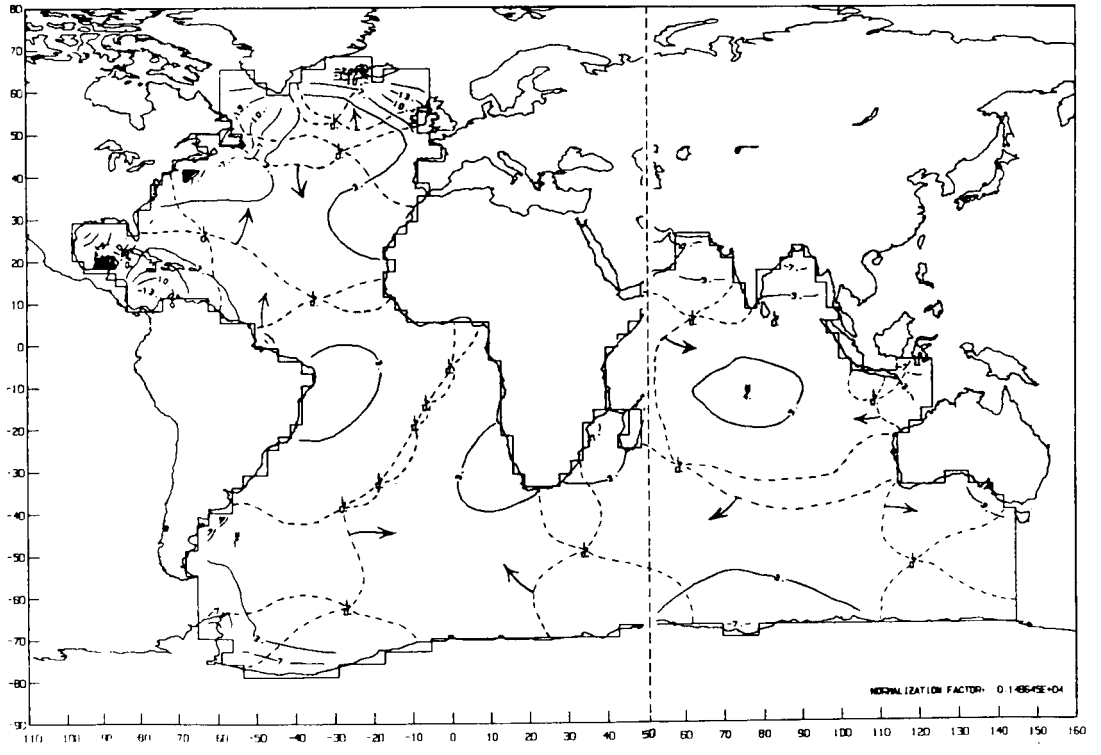

Figure 6. Normal Mode, Period = 11.10 hours

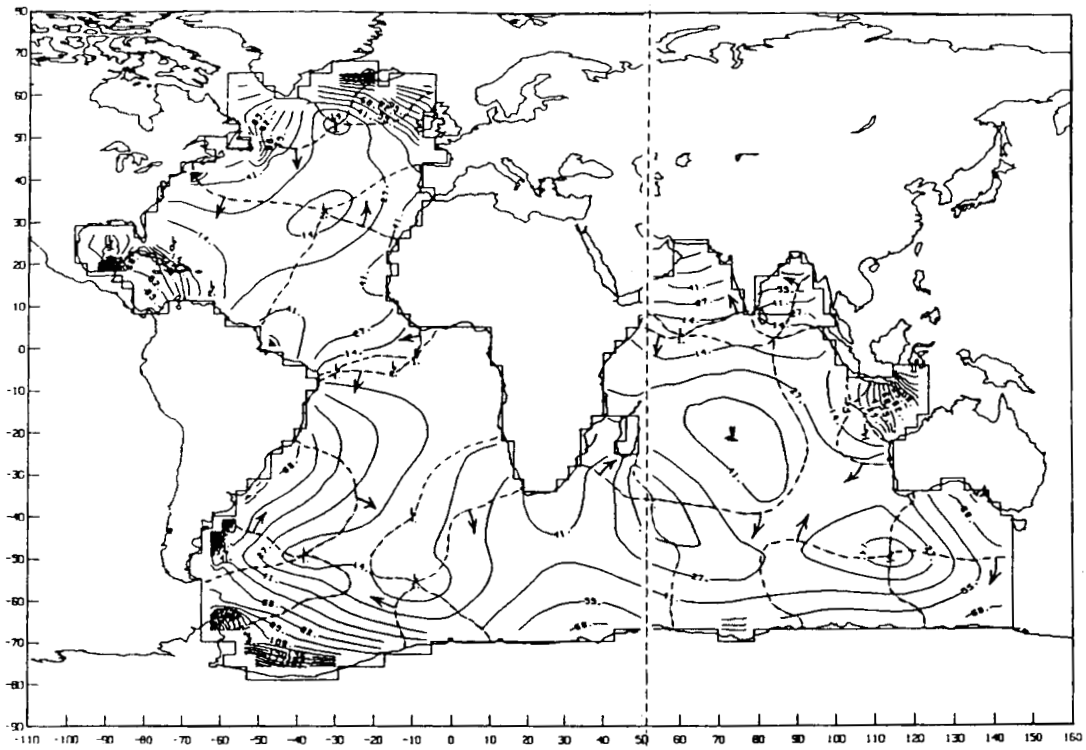

Figure 7. M2 Tidal Solution

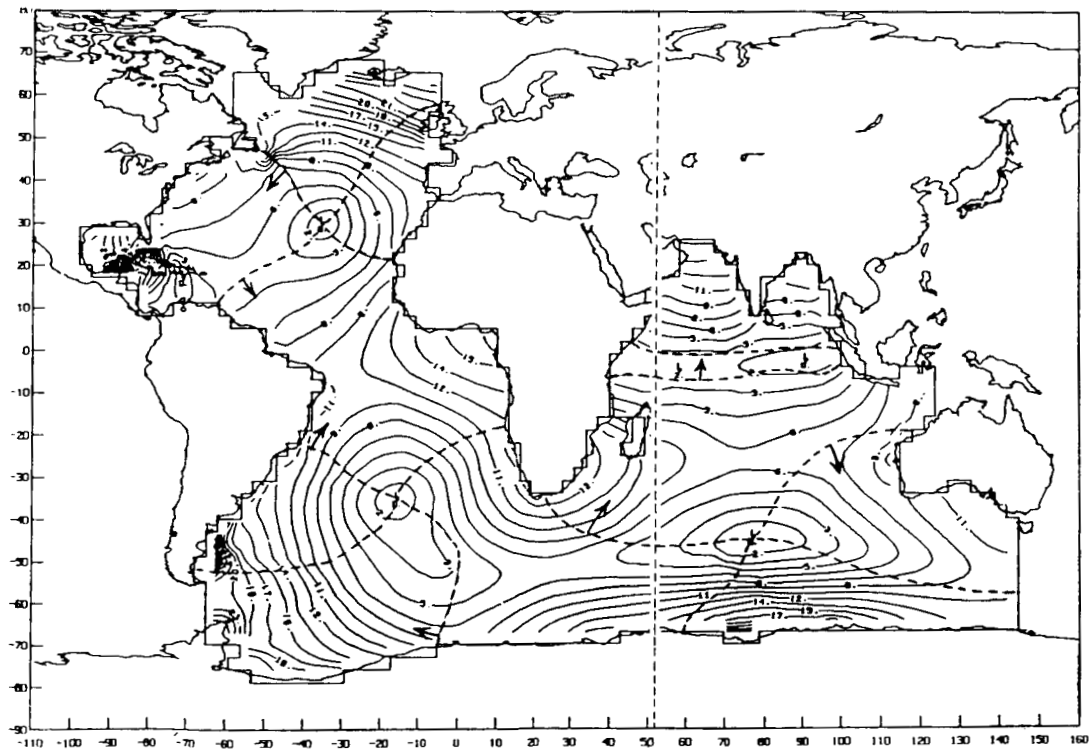

Figure 8. K1 Tidal Solution

Fitting the M2 Solutions by Mazzega and Schwiderski

The first effort to estimate the deep ocean tides from satellite altimeter data was done by Mazzega (1985). He used the SEASAT data to obtain a spherical harmonic expansion for the M2 tide in the world oceans. Mazzega's solution reproduces many of the features predicted by the present numerical models, therefore a fit to his solution using Proudman functions should be of some interest. We have used Mazzega's spherical harmonics coefficients to create values of amplitude and phase for the M2 tide at the 1915 points of our grid. We have used his expansion to degree and order 6; the resulting tide is shown in Figure 9 below.

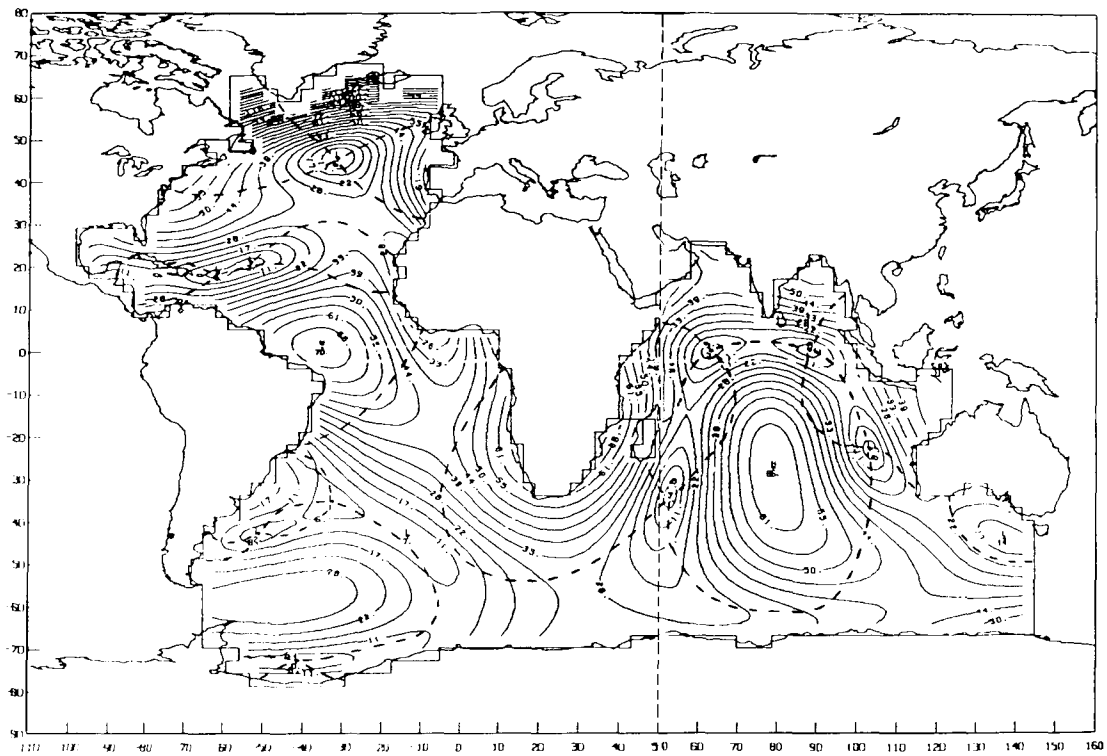

Figure 9. Mazzega's M2 Tidal Solution

The RMS in sea surface height-difference between our theoretical solution (150 functions) and Mazzega's solution is 39.06 cm before the fit. We then used the 1915 data points to estimate 150 coefficients which were used to create a fit to Mazzega's solution. The RMS in sea surface height-difference between the fit and Mazzega's solution is 3.91 cm. Letting 1915 represent 100%, the amplitude results are 539 points (28.14%) with fits within 5%, 1054 (55.03%) with fits within 10% and 1525 points (79.63%) with fits within 20% of the Mazzega's amplitude. The results for the phase are 650 points (33.94%) within 5 degrees, 1425 points (74.41%) within 10 degrees and 1749 points (91.33%) within 20 degrees of the phase values given by Mazzega. Figure 10 shows the contours of amplitude difference (cm) between the fit and Mazzega's solution.

Schwiderski's M2 solution was obtained from a tape where the values of amplitude and phase are specified on a $1^\circ \times 1^\circ$ grid; this grid is not congruent with the $3^\circ \times 3^\circ$ grid used in the generation of the Proudman functions; there is a separation of a quarter of a degree in latitude and longitude between the points in the two grids. This separation was considered small for the purpose of our test and the values of amplitude and phase at the closest point of the $1^\circ \times 1^\circ$ grid were simply adopted as the values in the $3^\circ \times 3^\circ$ grid. Figure 11 below shows the result.

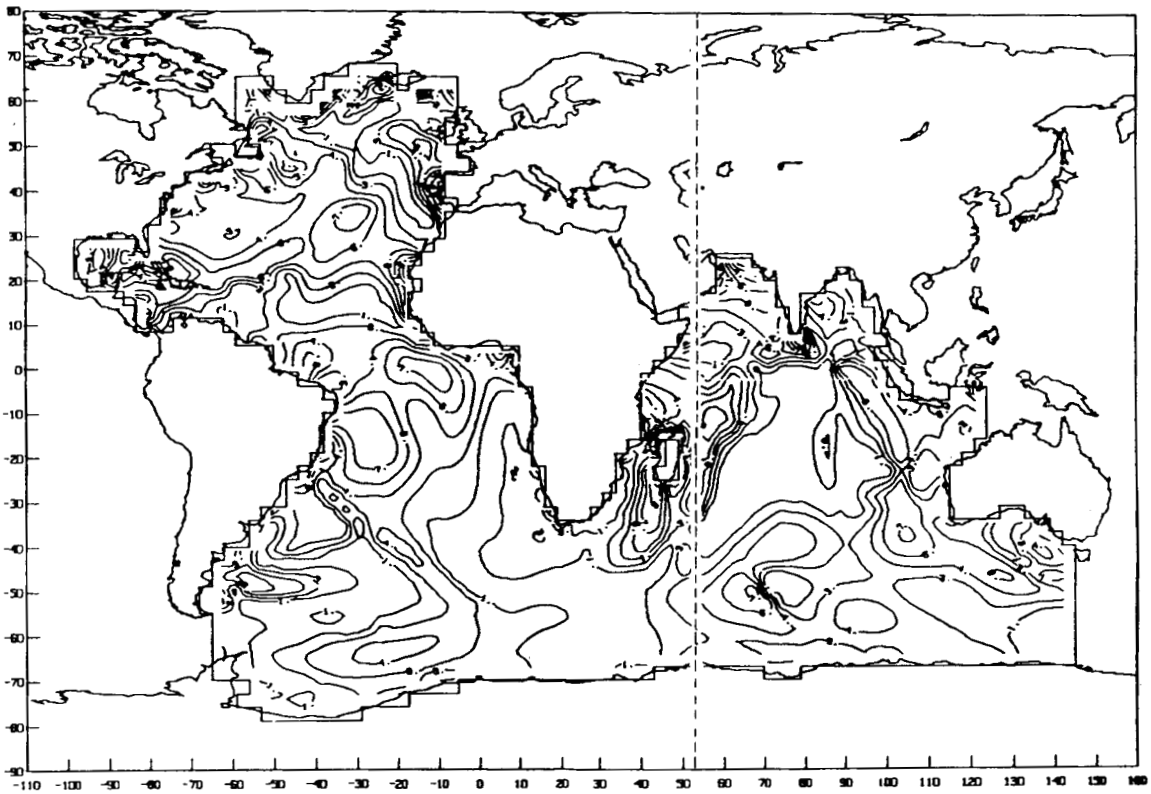

Figure 10. Amplitude Difference After Fitting Mazzega's M2 Tide with 150 Proudman's Functions

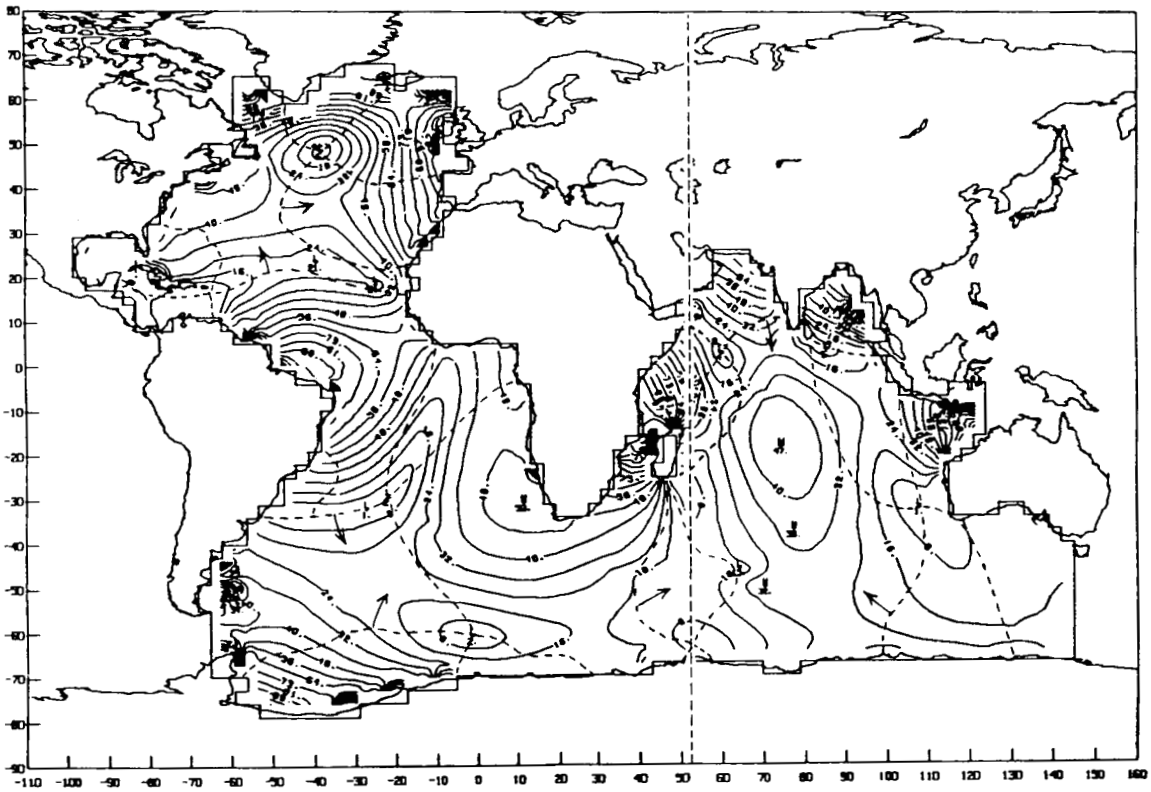

Figure 11. Schwiderski's M2 Tidal Solution

The RMS in sea surface height-difference between our theoretical solution and Schwiderski's solution is 33.93 cm before the fit. A fit to Schwiderski's solution is then obtained by estimating 150 coefficients from the 1915 data points. The RMS in sea surface height-difference between the fit and Schwiderski's solution is 6.53 cm. The amplitude results are as follows: 869 points (45.3%) with fits within 5%, 1356 points (70.8%) with fits within 10% and 1711 points (89.3%) with fits within 20% of Schwiderski's amplitude. The phase results are 1479 points (77.2%) within 5 degrees, 1705 points (89.0%) within 10 degrees and 1826 points (95.3%) within 20 degrees of the phase values given by Schwiderski. Figure 12 shows the contours of amplitude difference (cm) between the fit and Schwiderski's solution.

Spherical harmonics were also used to compute fits to Schwiderski's M2 solution. For an expansion of degree = 7, involving 128 coefficients, the RMS in sea surface height difference is 10.7 cm. The fit gets better with increasing degree, for an expansion of degree = 14 (450 coefficients) the RMS is down to 7.36 cm. Figure 13 shows the contours of amplitude difference (cm) between this last case and Schwiderski's solution.

An examination of Figures 12 and 13 indicates that most of the error for both fits occurs in the boundaries of the ocean basin, certain areas being more critical than others. The highest errors occur in the Labrador Sea, the Northeast Atlantic, the Mozambique Channel, the Bay of Bengal, the Timor Sea, the Weddell Sea and in the spherical harmonic fit: the Patagonian Shelf. The artificial closure along the Tasman Plateau shows little error in both cases.

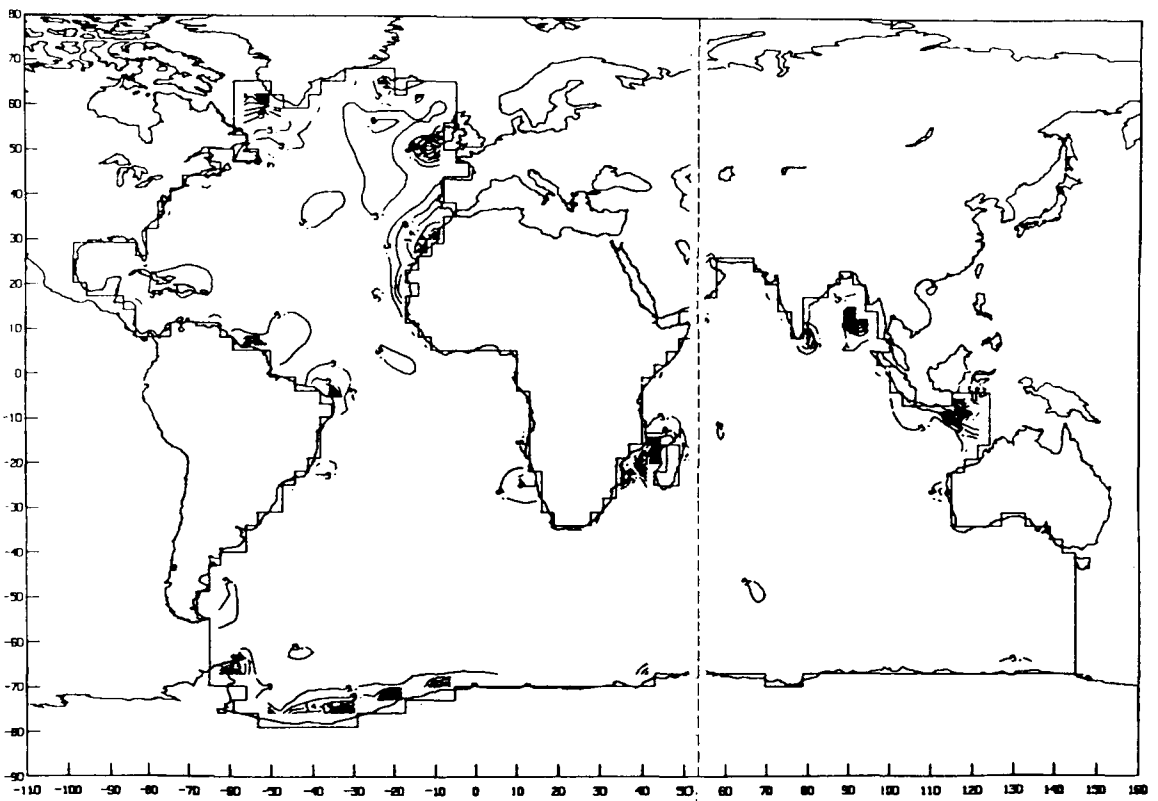

Figure 12. Amplitude Difference After Fitting Schwiderski's M2 Tide with 150 Proudman's function

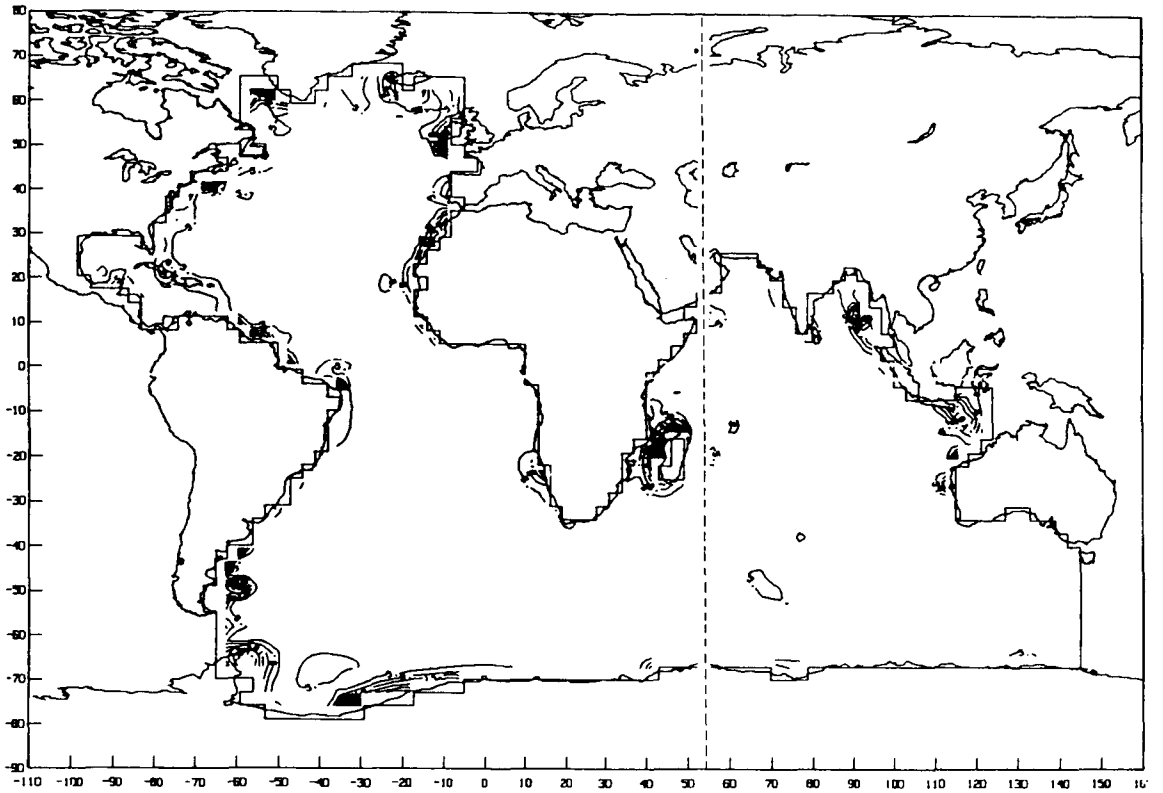

Figure 13. Amplitude Difference After Fitting Schwiderski's M2 Tide with a 14th-degree Spherical Harmonic Expansion

5. CONCLUSIONS

The stream function and velocity potential orthogonal functions were computed numerically in the Atlantic-Indian Ocean basin using a 3° x 3° finite difference grid and a Lanczos procedure. These solutions were used to obtain the normal modes of the basin and the results were compared with those obtained previously using a 6° x 6° grid. The Laplace Tidal Equations were used to obtain the forced solutions for the M2 and K1 tidal components; these solutions do not include friction, self-attraction of the tide or tidal loading. A power spectrum for the M2 and K1 components was obtained, showing which modes are the most energetic.

The eigenfunctions of the velocity potential were used to obtain fits to both Mazzega's and Schwiderski's solutions for the M2 tidal component. Using 150 functions Mazzega's solution was fit with RMS = 3.91 cm in sea surface height-difference. Schwiderski's solution was fit with RMS = 6.53 cm; this is still lower than a 14th degree fit using spherical harmonics which yields RMS = 7.36 cm and involves three times the number of coefficients (450).

ACKNOWLEDGMENTS

We would like to thank Melissa Harper and Beatrice Boccucci, Goddard Space Flight Center, for providing efficient secretarial support. We express our appreciation to Dr. Ronald Estes of SAR for providing us with the software used in the spherical harmonics computations and to Dr. Clyde Goad (formerly with NGS) for providing the tape containing Schwiderski's tidal solution.

REFERENCES

Mazzega, P., 1985. "M2 model of the global ocean tide derived from SEASAT altimetry." *Marine Geodesy*, 9.

Platzman, G.W., 1975. "Normal modes of the Atlantic and Indian Oceans." *J. Phys. Oceanography*, 5.

Platzman, G.W., 1984. "Normal modes of the world ocean. Part IV: Synthesis of diurnal and semidiurnal tides." *J. Phys. Oceanography*, 14.

Proudman, J., 1918. "On the dynamical equations of the tides." *Proceedings of the London Mathematical Society*, 18.

Rao, D.B., 1966. "Free gravitational oscillations in rotating rectangular basins." *J. Fluid Mech.*, 25.

Rao, D.B. and Schwab, D.J., 1976. "Two-dimensional normal modes in arbitrary enclosed basins on a rotating earth: application to Lakes Ontario and Superior." *Phil. Trans. Roy. Soc. (London)*, (A), 281.

Rao, D.B. and Schwab, D.J., 1981. "A method of objective analysis for currents in a lake with application to Lake Ontario." *J. Phys. Oceanography*, 11.

Sanchez, B.V., D.B. Rao and P.G. Wolfson, 1985. "Objective analysis for tides in a closed basin." *Marine Geodesy*, 9.

Sanchez, B.V., D.B. Rao, and S.D. Steenrod, 1986 a. "Objective analysis of tidal fields in the Atlantic and Indian Oceans." NASA TM 87773.

Sanchez, B.V., D.B. Rao, and S.D. Steenrod, 1986 b. "Tidal Estimation in the Atlantic and Indian Oceans." *Marine Geodesy*, 10.

Woodworth, P.L. and Cartwright, D.E., 1986. "Extraction of the M2 ocean tide from SEASAT altimeter data." *Geophys. J. R. astr. Soc.*, 84.

BIBLIOGRAPHIC DATA SHEET

1. Report No.	2. Government Accession No.	3. Recipient's Catalog No.
NASA TM-87812		

4. Title and Subtitle	5. Report Date
TIDAL ESTIMATION IN THE ATLANTIC AND INDIAN OCEANS, 3° x 3° SOLUTION	April 1987
	6. Performing Organization Code: 621
7. Author(s): Braulio V. Sanchez, Desiraju B. Rao, and Stephen D. Steenrod	8. Performing Organization Report No.: 87B0163
9. Performing Organization Name and Address: Goddard Space Flight Center, Greenbelt, MD 20771	10. Work Unit No.
	11. Contract or Grant No.
	13. Type of Report and Period Covered: Technical Memorandum
12. Sponsoring Agency Name and Address: National Aeronautics and Space Administration, Washington, D.C. 20546	14. Sponsoring Agency Code

15. Supplementary Notes

Braulio V. Sanchez: Goddard Space Flight Center, Greenbelt, Maryland.
Desiraju B. Rao: National Oceanic and Atmospheric Administration, National Meteorological Center, Rockville, Maryland.
Stephen D. Steenrod: Applied Research Corporation, Landover, Maryland.

16. Abstract

An estimation technique has been developed to extrapolate tidal amplitudes and phases over entire ocean basins using existing gauge data and the altimetric measurements which are now beginning to be provided by satellite oceanography. The technique was previously tested in the Lake Superior basin by Sanchez, Rao and Wolfson (1985) and in the Atlantic-Indian Oceans (using a 6° x 6° grid) by Sanchez, Rao and Steenrod (1986 a, b). Some results obtained by using a 3° x 3° grid are now presented.

The functions used in the interpolation are the eigenfunctions of the velocity potential (Proudman functions) which are computed numerically from a knowledge of the basin's bottom topography, the horizontal plan form and the necessary boundary conditions. These functions are characteristic of the particular basin.

The gravitational normal modes of the basin are computed as part of the investigation; they are used to obtain the theoretical forced solutions for the tidal constituents. The latter can provide the simulated data for the testing of the method and serve as a guide in choosing the most energetic functions for the interpolation.

17. Key Words (Selected by Author(s))	18. Distribution Statement
tidalfields, normal modes, M2, K1, Atlantic Ocean, Indian Ocean, ocean basins	Unclassified–Unlimited Subject Category 48

19. Security Classif. (of this report)	20. Security Classif. (of this page)	21. No. of Pages	22. Price*
Unclassified	Unclassified	20	A02

*For sale by the National Technical Information Service, Springfield, Virginia 22161

NASA-Langley, 1987